

## Effective Long-term Monitoring Strategies by Integrating Reactive Transport Models with In situ Geochemical Measurements – 16212

Haruko Wainwright \*, Boris Faybishenko \*, Sergi Molins \*, James Davis \*, Bhavna Arora \*, George Shu Heng Pau \*, Jeffrey Johnson \*, Greg Flach \*\*, Miles Denham \*\*, Carol Eddy-Dilek \*\*, David Moulton \*\*\*, Konstantin Lipnikov \*\*\*, Carl Gable \*\*\*, Terry Miller \*\*\*, Erin Barker \*\*\*\*, Vicky Freedman \*\*\*\*, Mark Freshley \*\*\*\*

\* Lawrence Berkeley National Laboratory

\*\* Savannah River National Laboratory

\*\*\* Los Alamos National Laboratory

\*\*\*\* Pacific Northwest National Laboratory

### ABSTRACT

Long-term monitoring of contaminant transport in groundwater is expected to account for a large fraction of future life-cycle cleanup costs at the DOE sites. The Attenuation-Based Remedies in the Subsurface Applied Field Research Initiative (ABRS AFRI) is developing an innovative approach for cost-effective *in situ* long-term monitoring. The approach is based on strategically adding the measurements of controlling variables (such as pH, redox potential, electrical conductivity, and groundwater level), which control the plume mobility and its spatial and temporal distribution. *In situ* measurements of these variables – supplemented with a reduced number of standard periodic groundwater samples – are expected to lead to more cost-effective monitoring, and can also serve as an early warning system for detecting unexpected plume migration.

The objective of this study is to support the development of such a long-term monitoring approach through the application of advanced computational methods, including (1) statistical data mining and analysis, and (2) three-dimensional flow and reactive chemical transport modeling. We have performed the statistical data analysis of historical and current monitoring data at the Savannah River Site (SRS) F-Area to quantify the correlations between the controlling variables and radioactive contaminant concentrations. In parallel, we have used 3D modeling of flow and contaminant transport to provide the prediction of the contaminant plume evolution. The results of both data analysis and modeling confirmed that the correlations between controlling variables and contaminant concentrations are significant. Modeling results also suggest that the correlation parameters will change in the future, which is important to assess the long-term efficacy of the proposed monitoring approach.

### INTRODUCTION

Nuclear weapon production during the Cold War has resulted in groundwater contamination at many locations in the United States. Low-level radioactive waste solutions were often disposed into unlined seepage basins with minimal or no engineered barriers. Remediation of these sites poses one of the most technically complex cleanup challenges in the world [1]. Although many remediation efforts have been successful or are expected to finish in the next several decades, continued

monitoring of groundwater will be required for decades at most of these sites – particularly the sites that have been selected for monitored natural attenuation – to ensure long-term safety. The current practice of monitoring – obtaining and analyzing the contaminant concentrations in groundwater samples at numerous wells – is quite costly especially over long time frames. The long-term monitoring is, in fact, expected to account for a large fraction of the life-cycle cleanup costs at the DOE sites.

To tackle this challenge, the Attenuation-Based Remedies in the Subsurface Applied Field Research Initiative (ABRS AFRI) is developing an innovative approach for cost-effective *in situ* long-term monitoring. This approach is based on strategically adding *in situ* measurements of controlling variables (such as pH, redox potential, groundwater level, and electrical conductivity) to the standard monitoring and groundwater sampling approach. Such variables control the plume mobility and its spatial and temporal distributions, and they can be measured *in situ*, using distributed automated sensors over time at a significantly lower cost compared to the standard groundwater sampling and analysis. Such an *in situ* sensor network, supplemented with a reduced number of standard periodic groundwater measurements, will lead to the development of more robust and cost-effective monitoring. In addition, it can serve as an early warning system for detecting the plume migration.

Critical to assessing such an *in situ* monitoring strategy over a long time frame is the predictive understanding of long-term plume mobility and its correlations with the controlling variables. Modeling of flow and contaminant transport enables the prediction of contaminant plume evolution under various conditions for many years. Simulation results can, for example, be used to explore the correlations between contaminant concentrations and controlling variables, providing the practical basis for using these such correlations for monitoring. In addition, modeling allows us to evaluate the long-term viability of the developed approach by predicting, for example, the effect of hydrological shift due to climate change, or the effect of operational decisions on monitoring.

In parallel to such mechanistic modeling, the use of data analytics is key for optimization of continuous-time monitoring data from distributed sensors; also historical datasets are invaluable for validation of modeling results and development of monitoring strategies. Recent rapid advancement in statistical methods and software allows us to discover hidden patterns and trends within the datasets. Particularly, a multivariate regression analysis can identify the temporal and spatial variability of correlations between the controlling variables and contaminant concentrations. In addition, cluster analysis can be used to group monitoring wells into clusters that behave similarly such that we can reduce the number of monitoring wells.

This integrated approach – combining mechanistic modeling from first principles, and data-driven statistical approaches – will enable us (1) to confirm consistency between data and models, (2) to improve our system understanding and (3) to iteratively build our confidence on the developed monitoring approach. This data-model integration, along with the developed monitoring approach, will be transformational for the

environmental monitoring programs at the DOE and other sites.

In this paper, we present our preliminary results of modeling and statistical analysis for the conditions of the Savannah River Site (SRS) F-Area, where groundwater was contaminated by acidic low-level waste solutions that were disposed of into unlined basins beginning in the 1950's. The plume contains various contaminants including uranium isotopes, Sr-90, I-129, Tc-99, and tritium, as well as nitrate. The SRS F-Area environmental compliance team has developed a robust and diverse historical database of characterization and monitoring data that include measurements from a large number of wells (including contamination concentrations, hydrological variables and other geological data) over time. These historical data enable us to explore the correlations between the controlling variables and contaminant concentrations, and also to test the developed approach in a historical manner.

A three-dimensional (3D) flow and reactive transport model has been developed at the SRS F-Area under the Advanced Simulation Capability for Environmental Management (ASCEM) project funded by DOE Office of Environmental Management (<http://esd1.lbl.gov/research/projects/ascem/>). ASCEM is an open source, modular computing framework that incorporates new advances and tools for predicting contaminant fate and transport in natural and engineered systems. ASCEM includes a state-of-art numerical code (Amanzi) on high-performance computing (HPC) platforms for simulating complex flow and reactive transport, and numerous toolsets such as data management, visualization, uncertainty quantification (UQ) and parameter estimation (PE). At the F-Area, the model has been used to evaluate different engineering treatment options [2]. The combination of these two components – data analysis and modeling– enables us to transform the F-Area to be a real/virtual test bed for DOE-EM applications.

This paper presents the preliminary results in our development. We first describe the site, and our data analysis and modeling approaches in detail. We then show the data analysis results and the simulation results from our 3D reactive transport model. Finally, we quantify the correlations between contaminant concentrations and controlling variables, as well as compare the correlations from two approaches for evaluating the consistency between the model and data.

## **SITE DESCRIPTION**

The Savannah River Site (SRS) is located in south-central South Carolina, near Aiken, approximately 100 miles from the Atlantic Coast. It covers about 800 km<sup>2</sup> (300 mi<sup>2</sup>) and contains facilities constructed in the early 1950s to produce special radioactive isotopes (e.g., plutonium and tritium) for the U.S. nuclear weapons stockpile. The SRS F-Area seepage basins were constructed as unlined, earthen surface impoundments that received ~7.1 billion liter of acidic, low-level waste solutions from the processing of irradiated uranium in the F-Area Separations facility from 1955 through 1988 [3]. Currently, an acidic contaminant plume extends from the basins ~600 m downgradient to the Four Mile Branch creek, including various radionuclides, such as uranium isotopes, Sr-90, I-129, Tc-99, tritium, and other contaminants, such as nitrate.

Various remediation activities have been conducted at the site, including capping of the basins (1991) and pump-and-treat (1997–2004). A hybrid funnel-and-gate system has been in operation since 2004, which includes low-permeability engineered flow barriers, and injection of alkaline solutions. The base injections are considered to be effective in neutralizing the acidic groundwater and in greatly increasing uranium retardation, since uranium mobility is significantly influenced by pH (because higher pH values increase uranium sorption). At the same time, the barriers slow down plume migration and increase decay and mixing before the plume reaches the Four Mile Branch creek, a down-gradient stream that ultimately captures the plume. Monitored Natural Attenuation (MNA) is a desired closure strategy for the site, assuming that infiltration of rainwater will eventually increase the pH of the plume, causing much stronger retardation and dilution of the uranium plume.

The hydrogeological conditions of the F-Area have been described in several previous studies [2, 4, 5]. SRS is located within the Atlantic Coastal Plain physiographic province, which is characterized by sub-horizontal sedimentary layers. There are three hydrostratigraphic units within the Upper Three Runs Aquifer: an upper aquifer zone (UUTRA), a Tan Clay Confining Zone (TCCZ), and a lower aquifer zone (LUTRA). Beneath the LUTRA is a clay layer called the Gordon confining unit. UUTRA and LUTRA are permeable sandy layers, and TCCZ is a low-permeable mixed sand-and-clay layer. The water table data suggest that TCCZ is a leaky confining unit so that UUTRA and LUTRA are hydrologically connected, while the Gordon confining unit is a semi-impermeable confining unit.

The geochemical conditions have been extensively characterized through many field and laboratory experiments, particularly for uranium geochemistry. In this paper, we focus on uranium chemistry, since mechanistic models have been developed to describe its sorption and pH-dependent behaviors. As described in Bea et al. [4], the natural attenuation of the acidic-U(VI) plume in the F-Area is likely to be affected mainly by the following processes: (1) adsorption/desorption of U(VI) onto/from the surface of different minerals (mainly kaolinite and goethite at this site) under different mechanisms (i.e., electrostatic surface complexation and/or ion exchange) [6]; (2) pH effects related to H<sup>+</sup> sorption and/or Al mineral dissolution and precipitation; (3) mixing of the plume groundwater with clean (and higher pH) background groundwater.

## **METHODOLOGY**

### **3D Flow Model Development**

A 3D reactive transport model has been continuously developed and improved over the last five years [2,7]. The 3D hydrological model was developed based on the previous flow model developed for a larger domain encompassing the overall General Separations Area (GSA) [5]. The water table computed in the GSA flow model was used to define a model domain that follows natural hydrologic boundaries (Fig. 1a). The domain includes three main hydrostratigraphic units: UUTRA, TCCZ and LUTRA.

Recent improvements focused on the hydrostratigraphic interfaces and engineered

barrier systems. The interfaces were updated based on recently acquired cone penetrometer testing datasets and surface seismic datasets [8], which capture the detail heterogeneity of the TCCZ top (or the lower boundary of UUTRA). The top of the TCCZ is known to be quite important for plume migration, since its depressions (or troughs) accumulate the contaminants (Fig. 1a). The new domain also includes low-permeability engineered barriers, which are part of the funnel-and-gate system (Fig. 1).

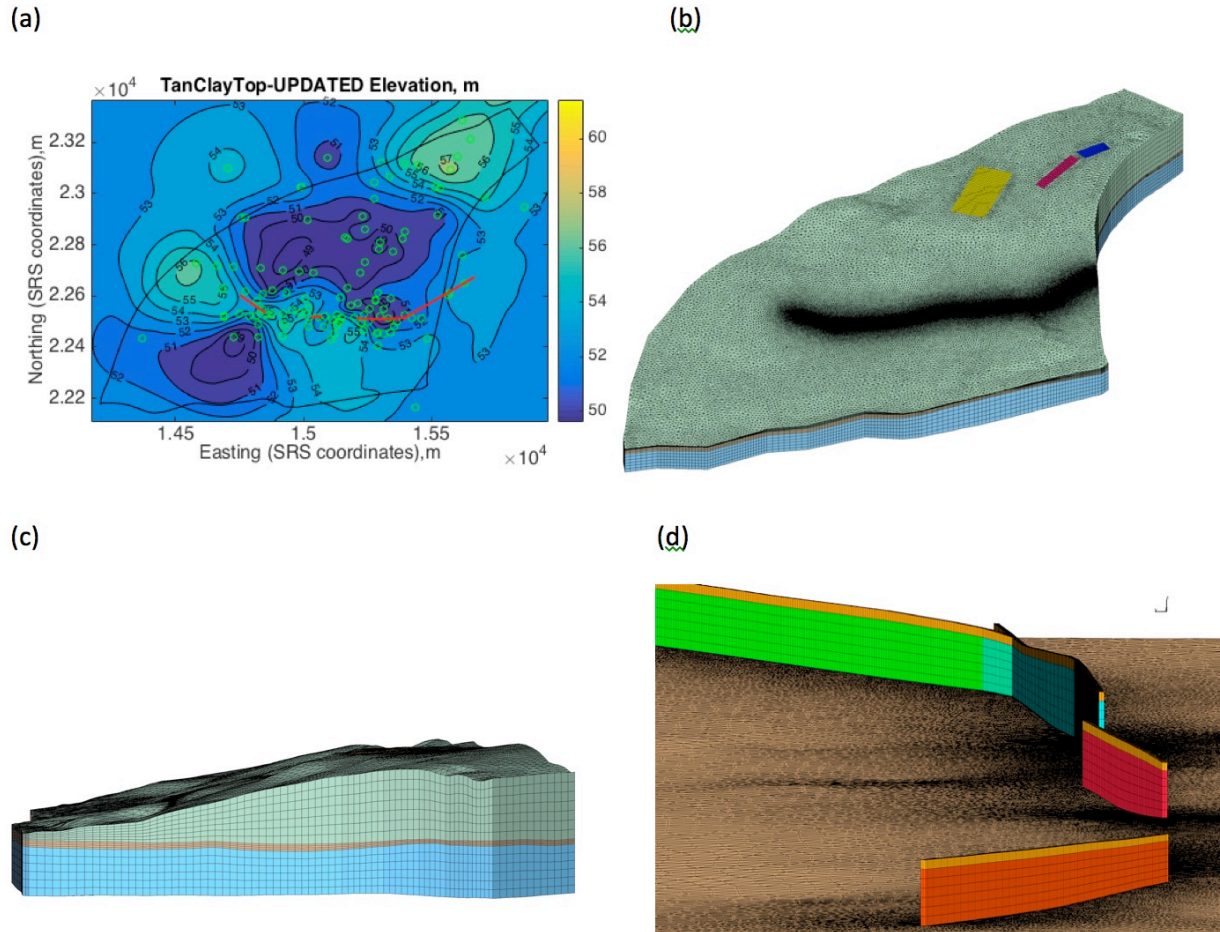


Figure 1. (a) Plan view of the 3D flow and transport domain with the contour plot of TCCZ depths, and (b-c) 3D prismatic mesh generated by LaGriT is shown using an exaggerated vertical scaling to highlight the three stratigraphic layers. In (a), the colored contour represents the water table computed in the GSA flow model, the red lines are the barrier locations, and the green circles are the base injection wells. In (b), the green region is the upper aquifer, the middle brown layer is the Tan Clay confining zone, and the blue region is the lower aquifer.

The unstructured 3D prismatic mesh was improved significantly using the Los Alamos Grid Toolbox (LaGriT; <http://lagrit.lanl.gov>; Fig. 1b-d). The mesh is refined around the barriers and basins, where we expect a sharp gradient in pressure and concentrations. Mesh edge lengths were smallest (highest resolution) at the barrier

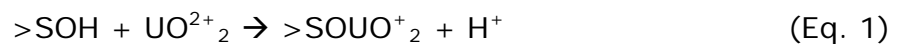
locations (Fig. 1d) with edge lengths near .2 meters. The regions with no small features to capture have larger spacing with edge lengths between 20 and 50 meters (Fig. 1b). The final mesh used in this study has 1,849,039 cells and 982,998 vertices, which is significantly more refined than the previous model [2].

The 3D flow and transport simulations were performed using the Richards equation and advective transport Process Kernels in Amanzi on the NERSC HPC platforms. The same aquifer properties as the two-dimensional flow model developed by [4] were used. A permeability of  $1 \times 10^{-17} \text{m}^2$  was assumed for the engineered barriers. The upstream model boundary was treated as fixed pressure based on the measured water-table height. The upper surface was treated as a constant recharge boundary with a moving seepage face to allow groundwater flow to upwell and discharge to the Four Mile Branch creek. The other boundary conditions were treated as no-flow, including the vertical boundary below the stream, the bottom boundary of the model which is a relatively continuous low-permeability clay layer, and sides of the model which are parallel to flow.

### 3D Reactive Transport Model Development

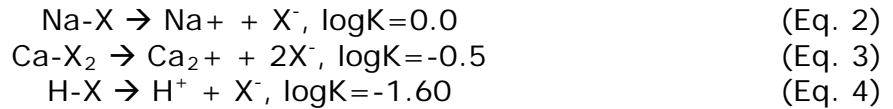
A three-dimensional reactive transport model was assembled by combining the flow and transport model detailed above and the geochemical model developed in the Phase II Demonstration [7]. The combination of the flow and transport portion of the model and the geochemical model was enabled by the Alquimia interface in Amanzi. This interface makes it possible to use existing geochemical codes (e.g. PFLTRAN, CrunchFlow) within the ASCEM HPC infrastructure through a generic coupling.

In the Phase II Demonstration [7], a geochemical model was developed based on part on the work of Bea et al. [4] as well as on a sorption model that relied on a single-site equilibrium, pH-dependent surface complexation. The primary geochemical system consists of 13 reactive chemical components and 8 minerals. The sorption model, however, provides the principal control on the uranium migration rate. An ion exchange model includes reactions involving the major cations ( $\text{Ca}^{2+}$ ,  $\text{Na}^+$ , and  $\text{Al}^{3+}$ , along with  $\text{H}^+$ ) and provides primary pH buffering along with the mineral reactions. The uranium mobility is controlled largely by a single sorption reaction, with the only significant effect on the stability of the surface complexation being the solution pH and carbonate activity. The pH has an effect directly through the surface complexation reaction:



where  $>\text{SOUO}_2^+$  refers to the uranium-bearing surface complex developed on the sediment grain surfaces. This nonelectrostatic model is applied to the bulk sediment rather than to specific pure mineral phases that serve as sorbents in electrostatic models. The effect of carbonate concentration on the strength of the uranium surface complex (and thus the mobility of the uranium) enters indirectly through the various (calcium)-uranium-carbonate complexes that form as a function of carbonate activity and pH. At the F-Area, a significant mass of the  $\text{H}^+$  ion is sorbed on mineral surfaces. This effect is treated with a set of cation exchange reactions that represent the pH

buffering via sorption on mineral surfaces (in addition to pH buffering by mineral dissolution and precipitation reactions) by the following:



In essence, these ion exchange reactions, along with the single uranium surface complexation reaction, captured much of the pH and carbonate activity effects on uranium mobility and had the additional advantage that they involve a much smaller list of adjustable parameters than is included in [4] or [6]. A detailed list of reactions and geochemical parameters is included in the Appendix E of [7].

### **Statistical Data Analysis Method**

The purpose of the statistical data analysis was to assess whether there are correlations between the radionuclide concentrations and master variables, such as nitrate concentration and pH. Statistical data analysis included the evaluation of correlations between the concentrations of uranium isotopes, <sup>14</sup>C, tritium, nitrate and pH, which were detected in groundwater samples. We assumed that the nitrate concentration is a proxy for electrical conductivity (EC) of groundwater, since nitrate dominates the other dissolved species at F-Area within the plume.

## **RESULTS**

### **Statistical Analysis of Geochemical Concentrations**

Fig. 2 illustrates time series of concentrations in Well FSC 79 from 1990 to 2009. These data were used to calculate the general statistics of concentrations and a correlation matrix given in TABLE I. In TABLE I, the correlation coefficients, with a significance level  $\alpha < 0.05$ , are given in bold. For example, reasonable correlations exist between the concentration of U-238 and U-233/234 and  $\text{NO}_3^-$ , and between tritium (H-3) and  $\text{NO}_3^-$ , as well as a reasonable (inverse) correlation exists between tritium and pH. As expected, excellent correlations exist between different uranium isotopes 238, 235, and 233/234.

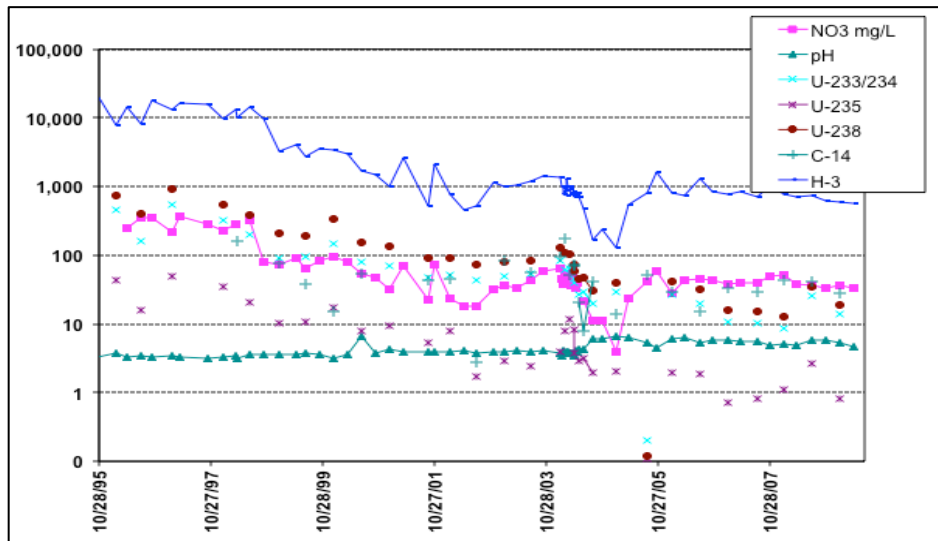


Figure 2. Time series of concentrations of radionuclides (all are in pCi/l), nitrate (in mg/l), and pH, which were used for the statistical analysis.

TABLE I. Correlation matrix of the concentrations of radionuclides, nitrate (NO<sub>3</sub>) and pH at FSB79.

Correlation matrix (Pearson)

Variables	NO <sub>3</sub> <sup>-</sup> mg/L	pH	<sup>233/234</sup> U pCi/L	<sup>235</sup> U pCi/L	<sup>238</sup> U pCi/L	<sup>14</sup> C pCi/L	<sup>3</sup> H pCi/L
NO <sub>3</sub> <sup>-</sup>	<b>1</b>	<b>-0.381</b>	<b>0.221</b>	0.177	<b>0.239</b>	<b>-0.229</b>	<b>0.700</b>
pH	<b>-0.381</b>	<b>1</b>	-0.125	-0.129	-0.158	0.105	<b>-0.477</b>
<sup>233/234</sup> U	<b>0.221</b>	-0.125	<b>1</b>	<b>0.956</b>	<b>0.970</b>	0.020	0.157
<sup>235</sup> U	0.177	-0.129	<b>0.956</b>	<b>1</b>	<b>0.951</b>	0.046	0.173
<sup>238</sup> U	<b>0.239</b>	-0.158	<b>0.970</b>	<b>0.951</b>	<b>1</b>	-0.003	<b>0.214</b>
<sup>14</sup> C	<b>-0.229</b>	0.105	0.020	0.046	-0.003	<b>1</b>	<b>-0.211</b>
<sup>3</sup> H	<b>0.700</b>	<b>-0.477</b>	0.157	0.173	<b>0.214</b>	<b>-0.211</b>	<b>1</b>

\* Values in bold are different from 0 with a significance level alpha=0.05

p-values

Variables	NO <sub>3</sub> <sup>-</sup>	pH	<sup>233/234</sup> U	<sup>235</sup> U	<sup>238</sup> U	<sup>14</sup> C	<sup>3</sup> H
NO <sub>3</sub> <sup>-</sup>	<b>0</b>	<b>0.000</b>	<b>0.031</b>	0.084	<b>0.019</b>	<b>0.025</b>	<b>&lt; 0.0001</b>
pH	<b>0.000</b>	<b>0</b>	0.223	0.210	0.124	0.307	<b>&lt; 0.0001</b>
<sup>233/234</sup> U	<b>0.031</b>	0.223	<b>0</b>	<b>&lt; 0.0001</b>	<b>&lt; 0.0001</b>	0.847	0.126
<sup>235</sup> U	0.084	0.210	<b>&lt; 0.0001</b>	<b>0</b>	<b>&lt; 0.0001</b>	0.659	0.092
<sup>238</sup> U	<b>0.019</b>	0.124	<b>&lt; 0.0001</b>	<b>&lt; 0.0001</b>	<b>0</b>	0.977	<b>0.036</b>
<sup>14</sup> C	<b>0.025</b>	0.307	0.847	0.659	0.977	<b>0</b>	<b>0.039</b>
<sup>3</sup> H	<b>&lt; 0.0001</b>	<b>&lt; 0.0001</b>	0.126	0.092	<b>0.036</b>	<b>0.039</b>	<b>0</b>

Values in bold are different from 0 with a significance level alpha=0.05

Fig. 3 presents scatter plots showing the regression between radionuclide concentrations and pH and radionuclides and nitrate concentrations. Fig. 3a shows that there is a complex relationship between concentrations of uranium isotopes and pH: as pH increases from 3.1 to ~5.5, uranium concentrations drop, and when pH increases to 6.5, uranium concentrations increase. Fig. 3b shows that the tritium concentration drops as pH increases from 3.1 to 4, and then the tritium concentration remains practically the same as pH increases. Fig. 3c demonstrates an excellent power-law regression between the tritium and nitrate concentrations, and Fig. 3d demonstrates satisfactory power-law regressions between uranium isotopes and nitrate concentrations.

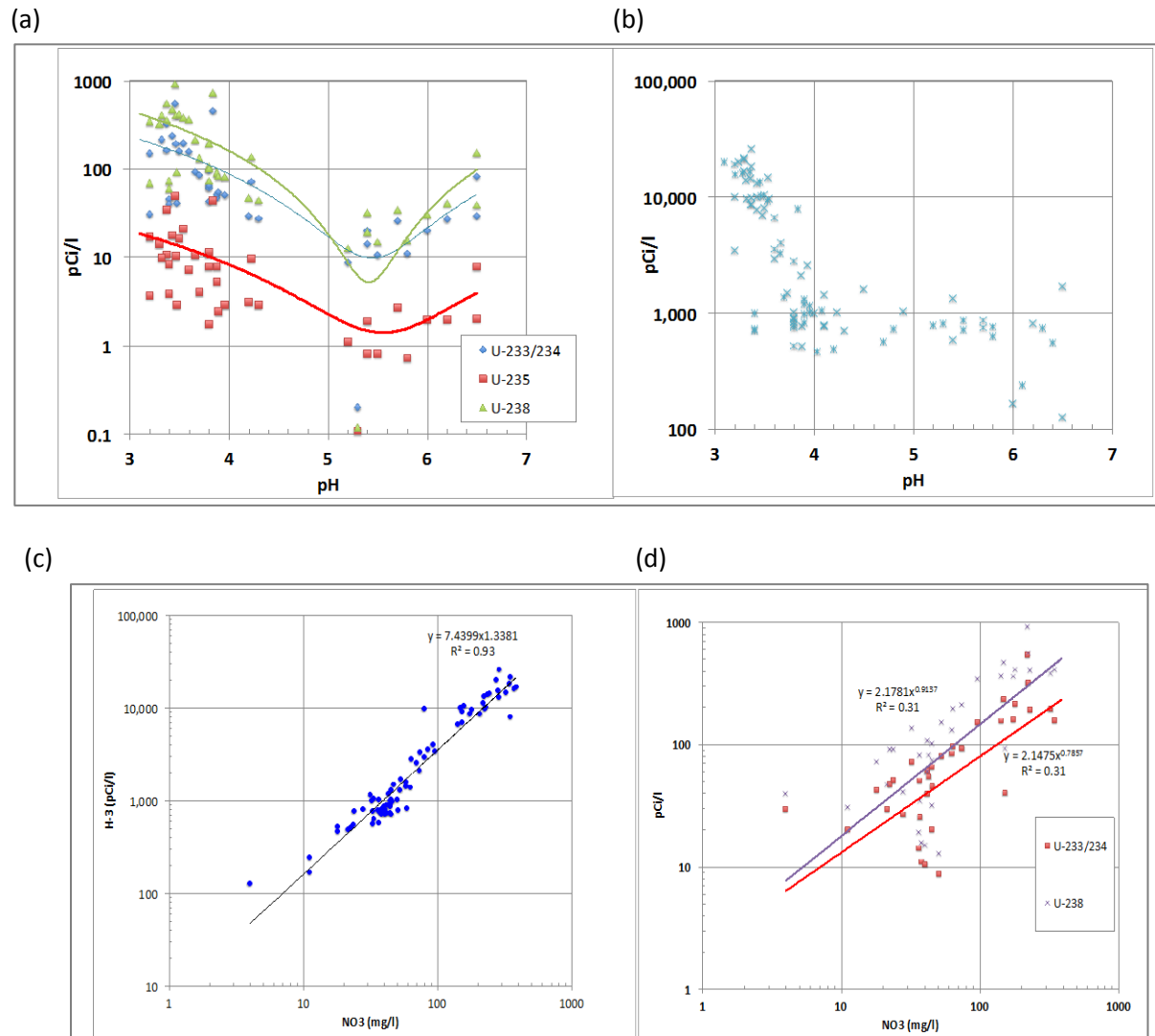


Figure 3. Graphical scatter plots of the regression at FSB79 between (a) radionuclide concentrations and pH, (b) tritium concentration and pH, (c) tritium concentration and nitrate concentration, and (d) uranium concentrations and nitrate concentration.

To evaluate the spatial variability of such correlations, Fig. 4 shows the observed correlations between uranium concentrations and controlling variables (electrical conductivity, pH and water table) at two wells in the upper aquifer (UUTRA): one near the source basin (FSB95D) and the other near the downgradient creek (FSB110D). The observation times are more limited than FSB 79 between 1993 and 2005. The points in Fig. 4 represent the observations after 1992, and considered to be at the trailing edge of the plume. The correlation coefficients and their *p* values are summarized in TABLE II. We observe a significant correlation between the controlling variables and the uranium concentration except for the water table at the downgradient well (FSB110D).

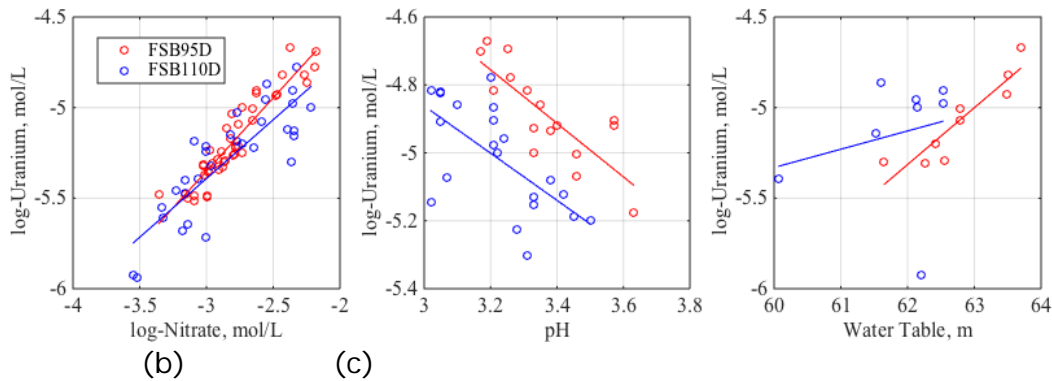


Figure 4. Observed correlations between uranium (U) concentration (log-transformed mol/L) and controlling variables at FSB95D and Well FSB110D: (a) nitrate concentration (log-transformed mol/L), (b) pH and (c) water table. In each plot, the lines are based on linear fitting of each time series.

TABLE II. The correlation coefficients (and their *p*-values) between the uranium concentration and master variables, shown in Fig. 4.

	FSB95DR	FSB110D
NO <sub>3</sub>	0.93 (<10 <sup>-4</sup> )	0.84 (<10 <sup>-4</sup> )
pH	-0.80 (2x10 <sup>-4</sup> )	-0.65 (0.0015)
Water Table	0.91 (5.94x10 <sup>-4</sup> )	0.23 (0.59)

Such strong correlations shown in Fig. 3 and 4 suggest the feasibility of inferring uranium concentrations based on the controlling variables, by describing the uranium concentration as a function of the master variables. Interestingly, the slope from linear (log – log) fitting (power-law function) is similar at two locations in the uranium-nitrate and uranium-pH correlations. It suggests that we may interpolate the functional parameters over the site based on sparse measurements. The correlations are, however, better for the well close to the source (FSB95D). It suggests the importance of quantifying the uncertainty at each location.

### 3D Flow and Reactive Transport Modeling Results

Fig. 5 shows the simulated evolution of the low-pH and uranium plumes. This simulation includes capping of the seepage basin, which limited the infiltration after the basin operation stopped. It does not include other remediation treatments at the site. The plumes initially move straight down vertically until they hit the water table, and then migrate laterally mainly within the upper aquifer (Fig. 5a and d). The low-pH plume moves more quickly down gradient (Fig. 5a and b), increasing the mobility of uranium and creating a way for the uranium plume to follow (Fig. 5d and e). As the plume migrates down gradient towards the creek, the plume goes through the troughs in the bottom of the upper aquifer (Fig. 5b). The model predicts that a significant amount of uranium is trapped in the vadose zone (Fig. 5f) in 2050 even though pH is neutralized (Fig. 5c), which suggests the long-term effect of capping the basin.

Fig. 6 shows the pH buffering caused by the dissolution of minerals present in the F-Area. This increase in pH reduces uranium mobility and minimizes the impact of discharging acidic solutions. In agreement with Bea et al., [4], kaolinite (and to a lesser extent goethite) dissolution during the seepage of acidic solutions provides the first pH buffering mechanism in the system (with 3 moles of  $H^+$  consumed for each mole of dissolved Al or Fe). Fig. 6b shows the extent of kaolinite depletion below the seepage basins. In addition to mineral dissolution, the retardation of the pH front with respect to conservative fronts is caused by the sorption of the cation  $H^+$  on the bulk mineral. Fig. 6c shows that indeed a significant mass of the  $H^+$  ion is sorbed on the mineral surfaces. In the absence of reactive mineral phases, this buffering mechanism would not exist and uranium would be more mobile and the concentrations higher.

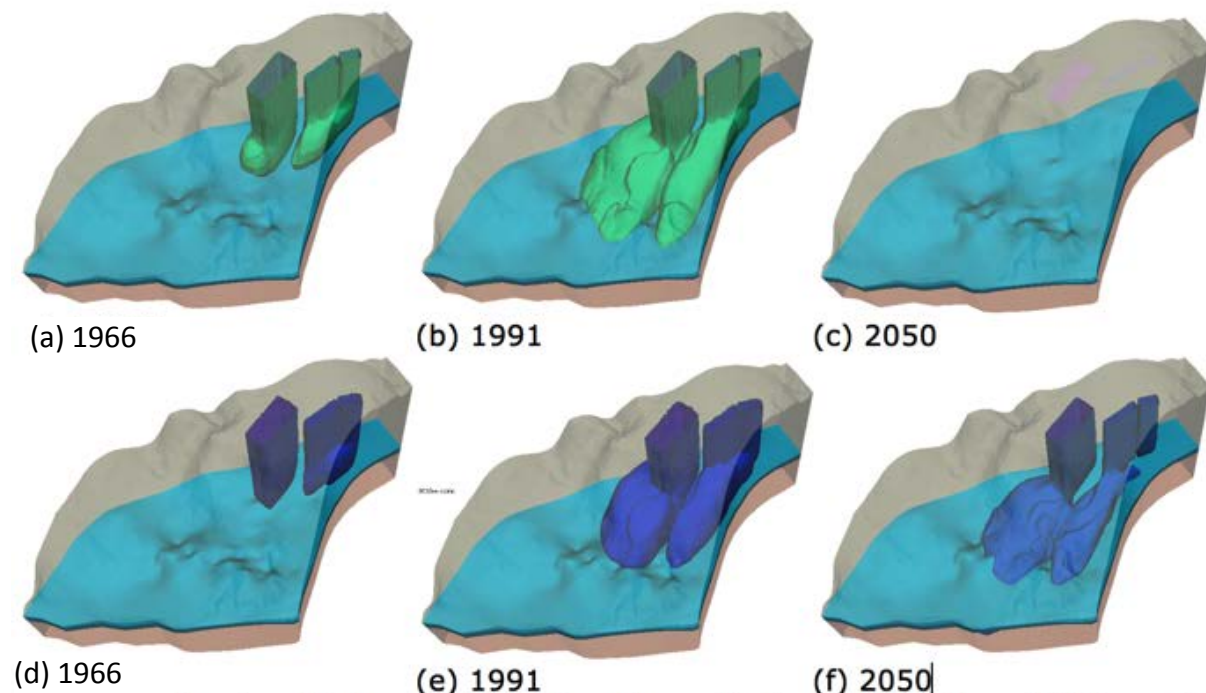


Figure 5. The simulated evolution of (a-c) low-pH plume (pH > 4) and (d-f) uranium plume (concentration >  $1 \times 10^{-6}$  mol/L). The sky blue region is the low permeable TCCZ, which separates the upper and lower aquifers. Vertical exaggeration = 15X.

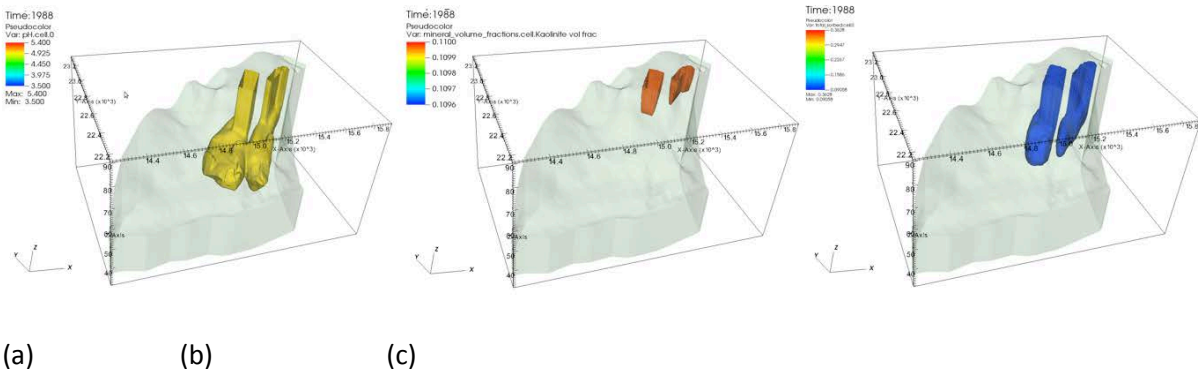


Figure 6: (a) low-pH plume represented as the pH 5 isosurface showing the extent of acidification below the seepage basins in 1988. (b) kaolinite-depleted zone as a result of dissolution driven by low pH conditions below the seepage basins in 1988, and (c) total sorbed concentration of  $H^+$  below the seepage basins in 1988 indicated as an isosurface at a concentration of  $0.1 \text{ mol/m}^3$ -bulk. Vertical exaggeration = 15X.

Fig. 7 shows the concentrations of three main species (uranium, aluminum and nitrate) at the same two wells as Fig. 4 (FSB95D near the basin and FSB110D near the down-gradient creek). Although the model is not fully calibrated yet at this time, the comparison to the observations shows a reasonable agreement particularly at FSB95D, which is close to the source basin. The agreement is comparable to the previous studies, using a two-dimensional reactive transport models [4, 6].

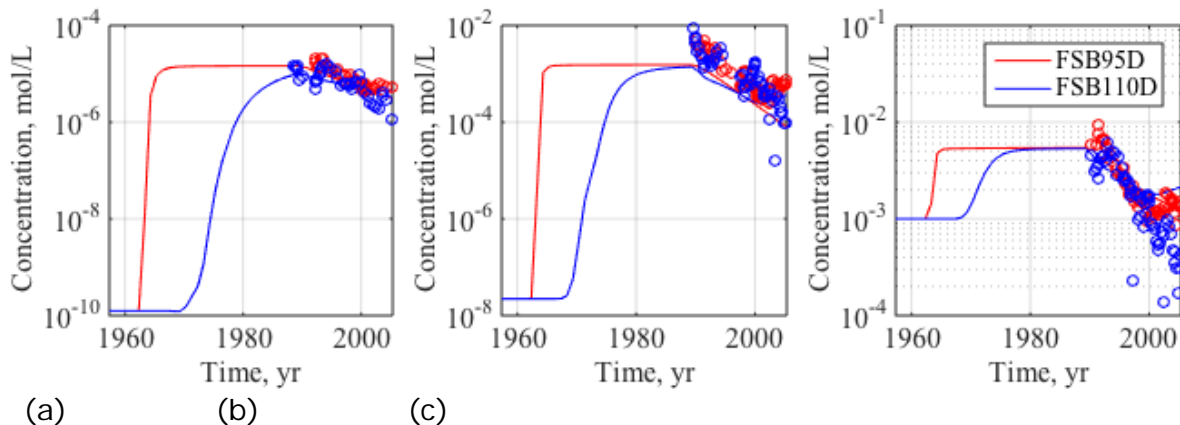


Figure 7: Comparison between the simulated concentrations (lines) and observations (circles) at FSB95D and FSB110D (a) uranium concentration ( $UO_2^+$ ), (b) aluminum concentration ( $Al^{3+}$ ) and (c) nitrate concentration ( $NO_3^-$ ).

Using these 3D reactive transport model results, we quantified the correlations between controlling variables (pH, water table, and electrical conductivity) and

contaminant concentrations (Fig. 8). As our preliminary results, we focused on the uranium concentration at the same two wells as Fig. 4 and 7. We assumed that the nitrate concentration is a proxy for electrical conductivity of groundwater. We selected the concentrations after 1992 corresponding to the observations (Fig. 4) but we also extended our predictions until 2100.

In Fig. 8, we see the correlations similar to the observations except for the water table (Fig. 4). We consider that the water-table correlation is different, because the current simulation assumes a constant recharge at the ground surface (without considering individual precipitation events). In addition, the current water table is approximate based on the pressure, which will be fixed in the near future. In the nitrate concentration (Fig. 8a) and pH (Fig. 8b), the predicted correlations are linear between 1993 and 2005, similar to the observations at the same wells, confirming the consistency between the model results and data. In addition, modeling also allows us to extrapolate the correlations into the future. The simulated results show that the pH-U correlations will be linear and constant until 2100, while the EC-U correlation will nonlinear and change over time.

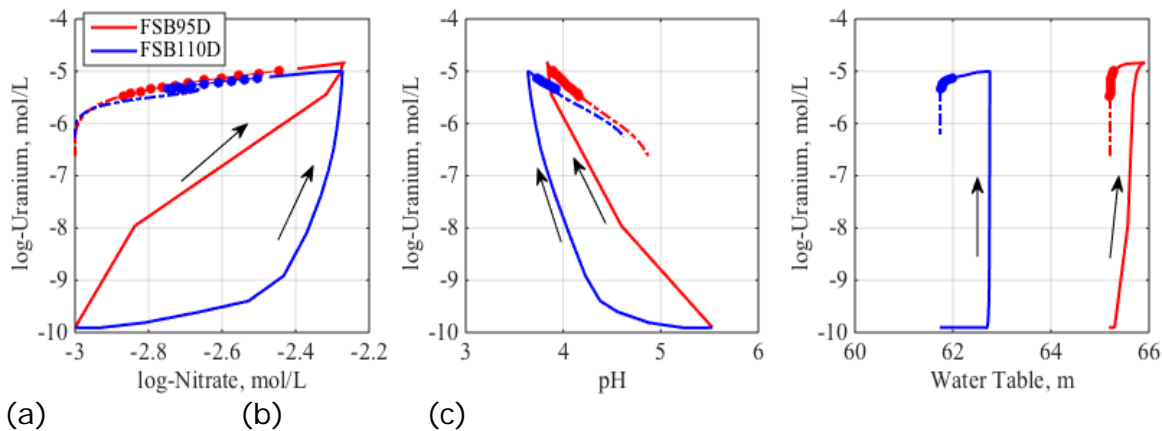


Figure 8. Simulated correlations between uranium (U) concentration (log-transformed mol/L) and controlling variables at FSB95D and Well FSB110D: (a) nitrate concentration (log-transformed mol/L), (b) pH and (c) water table. In each plot, the solid lines are between 1954 and 1993, the circles are between 1993 and 2005 (corresponding to the observations in Fig. 4) and the dotted lines are between 2005 and 2100. The black arrows in each plot represent the direction of the time evolution from 1954 to 2100.

## CONCLUSIONS

In this study, we demonstrated our combined modeling and statistical analysis approach to improve the long-term monitoring strategy at the SRS F-Area site. We developed a 3D flow and reactive transport model to describe the contaminant plume evolution in a mechanistic manner, including the complex pH-dependent reactions of uranium. In parallel, statistical analysis was applied to the historical datasets at the site to assess the correlations between radionuclide and nitrate concentrations and pH. Although our results are still preliminary, modeling results and data analysis

showed consistent correlations between controlling variables and uranium concentrations. These results confirm that the approach proposed by the ABRS-AFRI is promising for the long-term monitoring.

Our results showed that the uranium concentrations could be described as a function of controlling variables – particularly pH – measurable by in situ sensors. However, the parameters in the functions (such as the slope parameter in a linear model) depended on species, time and locations over the site. The uncertainty of those parameters was spatially and temporally variable as well. Our results suggest that the *in situ* sensors must be installed in groundwater monitoring wells over the site more strategically, and also occasional ground-truth measurements (i.e., groundwater sampling) are necessary to estimate those parameters accurately over time. It would be important that modeling and data analytics are in place at the site to iteratively validate and improve the monitoring approach over time.

Our future work will focus on improving this 3D model through parameter estimation and also including the water-table fluctuation as well as improved chemistry models for uranium and other species (particularly iodine). In addition, we will perform UQ to investigate the impact of the uncertainties and variability in hydrological and geochemical parameters, and also to predict the impact of the future hydrological shift. In parallel, we will use this model to evaluate the efficacy of the current or planned remediation treatments, and their impact on the long-term monitoring strategy.

### **ACKNOWLEDGEMENTS**

This study was supported as part of the ASCEM project, which is supported by U.S. Department of Energy, Office of Environmental Management, under the award number DE-AC02-05CH11231 to LBNL.

### **REFERENCE**

1. NRC, U.S. Department of Energy's Environmental Management Science Program: Research Needs in Subsurface Science. National Academy of Sciences: Washington, DC, 2000.
2. Wainwright, H.M., S. Molins, J.A. Davis, B. Arora, B. Faybishenko, H. Krishnan, S. Hubbard, G. Flach, M. Denham and C. Eddy-Dilek, J.D. Moulton, K. Lipnikov, C. Gable, T. Miller and M. Freshley, Using ASCEM Modeling and Visualization to Inform Stakeholders of Contaminant Plume Evolution and Remediation Efficacy at F-Basin Savannah River, SC, Proceedings of WM2015 Conference, Phoenix, Arizona, USA, March 15 – 19, 2015.
3. Killian, T.H., N.L., Kolb, P. Corbo, I.W. Marine, Environmental information document, F-Area seepage basins. Report No. DPST 85-704.E.I. du Pont de Nemours & Co, Savannah River Laboratory, Aiken SC 29808, 1986.
4. Bea, S. A., Wainwright, H., Spycher, N., Faybishenko, B., Hubbard, S. S., & Denham, M. E., Identifying key controls on the behavior of an acidic-U (VI) plume in the Savannah River Site using reactive transport modeling. Journal of contaminant hydrology, 151, 34-54, 2013.
5. Flach G., Groundwater Flow Model of the General Separations Area Using

- Porflow (U). WSRC-TR-2004-00106, Westinghouse Savannah River Company, Aiken, South Carolina, 2004.
6. Dong, W., T. Tokunaga, J. Davis, and J. Wan, *Environmental Science & Technology*, 46,1565–1571, 2012.
  7. Freshley, M. et al. *Advanced Simulation Capability for Environmental Management (ASCEM) Phase II Demonstration*, ASCEM-SITE-2012-01, 2012.
  8. Wainwright, H.M., J. Chen, D. Sassen and S.S. Hubbard, *Bayesian Hierarchical Approach for Estimation of Reactive Facies over Plume-Scales Using Geophysical Datasets*, *Water Resources Research*, 50, 4564–4584, doi: 10.1002/2013WR013842, 2014.